Picosecond to Second Dynamics Reveals a Structural Transition in *Clostridium botulinum* NO-Sensor Triggered by the Activator BAY-41-2272

Byung-Kuk Yoo,[†] Isabelle Lamarre,[†] Fabrice Rappaport,[‡] Pierre Nioche,[§] C. S. Raman,[‖] Jean-Louis Martin,[†] and Michel Negrerie*[,†]

[†]Laboratoire d'Optique et Biosciences, INSERM U696, CNRS UMR 7645, Ecole Polytechnique, 91128 Palaiseau Cedex, France
[‡]Institut de Biologie Physico-Chimie, UMR 7141 CNRS-UPMC, 13 rue Pierre et Marie Curie, 75005 Paris, France
[§]Laboratoire de Toxicologie et Pharmacologie, UMR S747, Centre Universitaire des Saints-Pères, 75006 Paris, France
[‖]Department of Pharmaceutical Sciences, School of Pharmacy, University of Maryland, Baltimore, Maryland 21201, United States

Ⓢ *Supporting Information*

ABSTRACT: Soluble guanylate cyclase (sGC) is the mammalian endogenous nitric oxide (NO) receptor that synthesizes cGMP upon NO activation. In synergy with the artificial allosteric effector BAY 41-2272 (a lead compound for drug design in cardiovascular treatment), sGC can also be activated by carbon monoxide (CO), but the structural basis for this synergistic effect are unknown. We recorded in the unusually broad time range from 1 ps to 1 s the dynamics of the interaction of CO binding to full length sGC, to the isolated sGC heme domain $\beta_1(200)$ and to the homologous bacterial NO-sensor from *Clostridium botulinum*. By identifying all phases of CO binding in this full time range and characterizing how these phases are modified by BAY 41-2272, we show that this activator induces the same structural changes in both proteins. This result demonstrates that the BAY 41-2272 binding site resides in the $\beta_1(200)$ sGC heme domain and is the same in sGC and in the NO-sensor from *Clostridium botulinum*.
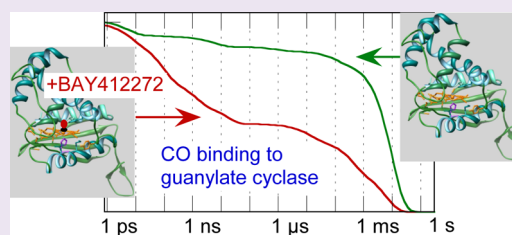
The soluble guanylate cyclase (sGC) is the receptor of the endogenous messenger nitric oxide (NO) in many cells. It catalyzes the formation of cGMP from GTP upon activation triggered by NO binding.[1,2] NO and sGC play a crucial role in several physiological processes: regulation of vascular blood pressure,[3] lung airway relaxation,[4] synaptic transmission, and immune response,[5] whose dysfunction results in cardiovascular,[3] inflammatory,[5] and pulmonary pathologies.[4] The NO-signaling pathway is also involved in tumor progression and apoptosis.[6] The high potential of sGC as a pharmacological target fostered the discovery of specific sGC activators,[7−11] which revealed the existence of an allosteric site in sGC.[12] In particular, the activator BAY 41-2272, elaborated from the first compound[10] YC-1, has been widely studied,[12] leading to the discovery of the cognate compound Riociguat (BAY 63-2521) whose pharmacokinetics is much more favorable.[8] These NO-independent activators induce the activation of purified sGC *in vitro* and a response of endothelium and smooth muscles cells from *ex vivo* isolated aorta rings[7,13,14] and elicit a reduction in blood pressure in experimental subjects;[12] however, there is no consensus on their mode of action on sGC at molecular level. A key observation is their action in synergy with CO[15,16] so that, in the simultaneous presence of CO and YC-1 or BAY 41-2272, sGC activation is not merely additive but similar to that obtained by NO alone.

The GTP binding and catalytic site, located at the interface, requires both the α- and β-subunits of the sGC heterodimer, whereas the regulatory β-subunit contains the heme cofactor necessary for NO binding and activation. The three-dimensional structure of sGC is unknown, but the heme domain structure of the β-subunit has been modeled from that of a bacterial NO-sensor[17,18] (named either H-NOX or SONO). The first molecular event leading to sGC catalytic activation is the cleveage of the heme iron-proximal His bond induced by NO binding. Because the sensing heme domain is harbored in a domain remote from the GTP catalytic site, activation must be mediated by a large-scale structural change, but the detailed activation mechanism is unknown. The synergistic activation[7] due to BAY 41-2272 and CO bound to the heme is expected to proceed through the same allosteric transition as that triggered by NO. Numerous mechanistic models of sGC activation have been proposed,[19−25] but contradictory results have been reported on the localization of activators binding site in sGC. Modeling studies,[26−28] mutations and activity assays,[26,27,29,30] and use of a photoactivable derivative of BAY 41-2272[12] led to localization of the activator binding site in the α_1-subunit
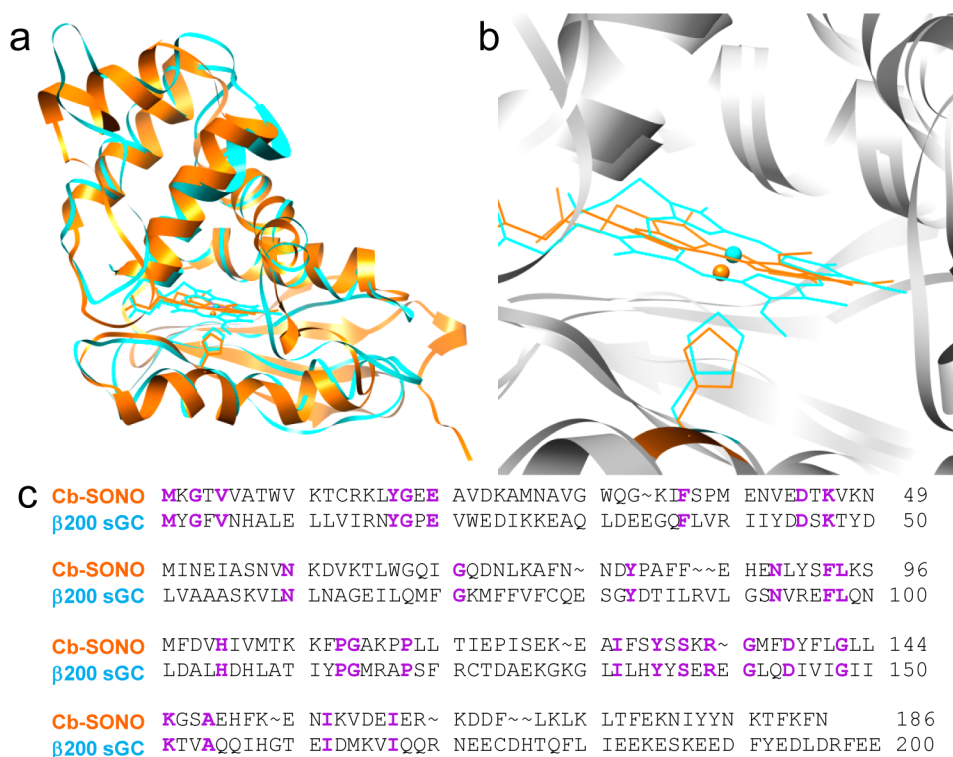
Figure 1. Structure and sequences of the two proteins studied. (a) Superposition of the *Cb*-SONO (orange) and the β_1(200) heme domain of sGC (cyan). Both structures result from homology modeling based on the crystal structure of the bacterial SONO heme domain from *Thermoanaerobacter tengcongensis* chemoreceptor protein. The energy of each molecule was minimized using CHARMM, and the superposition was performed using Chimera. (b) Close up view of the heme pocket. The heme and the proximal histidine are indicated as wires. (c) Multiple sequence alignment of the two proteins. Residues with strict identity are indicated in purple. Alignments were generated using BioEdit program.

(possibly at the interface with β_1-subunit), whereas no effect of YC-1 or BAY 41-2272 on β_1-heme domain constructs was reported.[21,31] Yet, Raman studies showed that the activators, in synergy with CO, perturb the heme pocket in full length sGC,[32−35] so that the issue of their binding site remained open.

In this work, we studied the structural transition induced in sGC by the activator BAY 41-2272 in synergy with CO using transient absorption spectroscopy[36−38] in order to locate the activator binding site and to demonstrate conformational changes. The rationale for this approach is that dynamics of all diatomics (O_2, CO, and NO) are highly sensitive to conformational changes because they modulate the energy barriers within the protein[38−41] and depend upon the allosteric states of the protein, so that if BAY 41-2272 changes the sGC allosteric state, we expect a change of CO dynamics in all time scales. We measured the CO dynamics in the broadest possible time range, encompassing 12 decades from picosecond to second, in the full-length dimeric sGC, in the isolated sGC heme domain β_1(200), and in a bacterial heme protein from *Clostridium botulinum*[17] to identify effects of the activator in their NO-sensing heme domain. The putative NO-sensor from *C. botulinum* (186 amino acids in length, hereafter abbreviated as *Cb*-SONO) is associated with a methyl-accepting chemotaxis protein and is homologous to the sGC heme domain (Figure 1). The comparison between both proteins is motivated by the similarity of their tertiary structure and sequence and by the starting hypothesis that a binding site for BAY 41-2272 activator may also exist in SONO heme domains. We thus compared the effect induced in sGC *versus* that induced in *Cb*-SONO and the isolated β_1(200) heme domain of sGC.

We probed the heme pocket conformation by monitoring at the same time CO geminate rebinding (in the ps−ns time range) and CO bimolecular rebinding from solvent (μs−ms time range; k_{on} rates) to probe large scale effects of BAY 41-2272. The ligand CO was chosen instead of NO because the latter geminately rebinds very quickly to sGC (7.5 ps)[36] with high efficiency (97%)[36] and can hardly be used as a probe of internal dynamics on time scales larger than 100 ps. Second, CO does activate sGC in synergy with BAY 41-2272. The investigation of the NO-sensor from *Cb*-SONO allows the direct comparison with the sGC heme domain, which has the same tertiary structure, and clearly demonstrates that this NO-sensor is subject to induced conformational changes. This last point is important because *Cb*-SONO has the highest affinity for NO so far measured and is coupled to a methyl-accepting chemotaxis domain[17] that is expected to be involved in the survival of the bacteria.

■ **RESULTS AND DISCUSSION**

Steady-State Interaction of BAY 41-2272 with sGC and *Cb*-SONO. The binding of the effector BAY 41-2272 to the full-length sGC in its resting state, without diatomic ligand bound to the 5-coordinate heme, induces a ∼1-nm shift of the Soret absorption band (from 432 to 431 nm; Figure 2a). A shift (2.6 nm) is similarly observed in the case of the binding of BAY 41-2272 to the homologous NO-binding domain *Cb*-SONO (Figure 2c). In agreement with the Soret band behavior, a shift (2−3 nm) of the Q-bands (α and β) maxima (in the 530−570 nm range) occurs in the absence of CO upon binding of BAY 41-2272 to the proteins (Figure 2b and d).
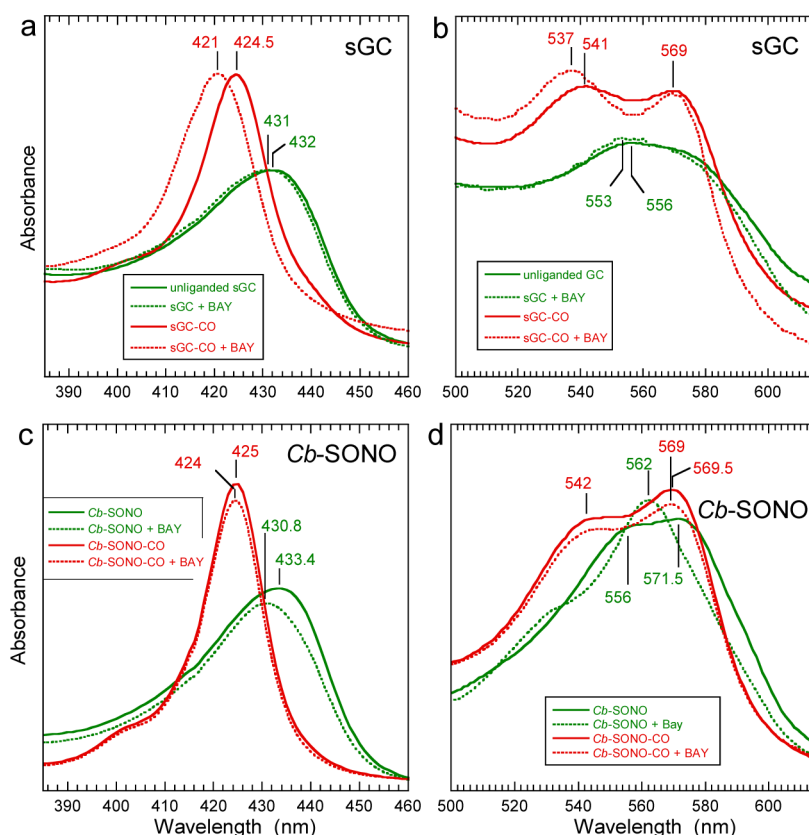
Figure 2. Steady-state absorption spectra of sGC (a,b) and *Clostridium botulinum* NO-sensor (c,d). The comparison of the Soret band (a and c) and the Q-bands (b and d) reveals the changes induced by the binding of CO to the heme (red lines) with respect to unliganded heme (green lines) and by the binding of activator BAY 41-2272 (dotted lines) with respect to its absence (solid lines). The spectra were normalized for dilution due to the addition of BAY 41-2272.
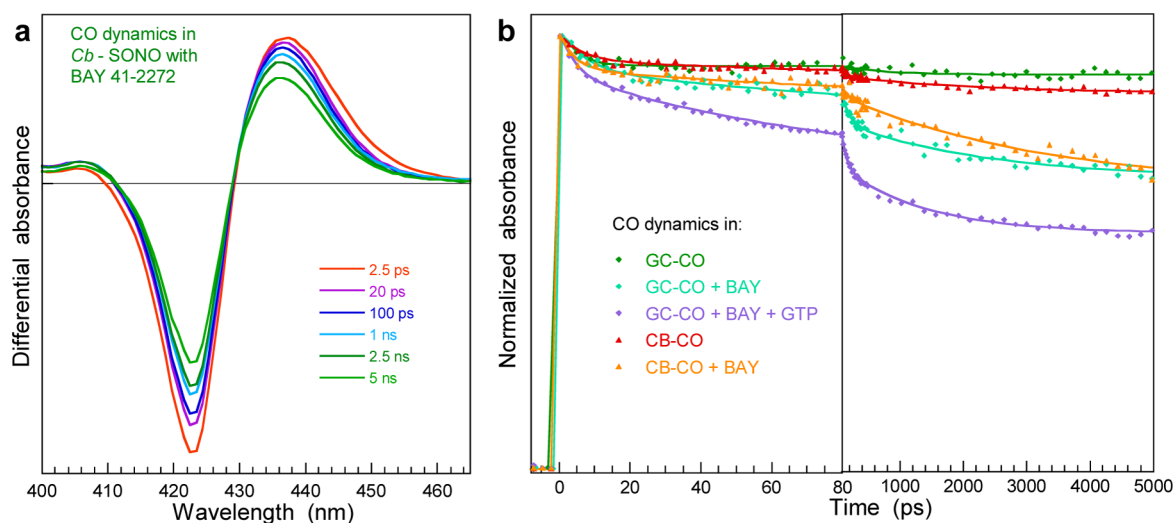
Figure 3. Changes in CO dynamics (1 ps to 5 ns time range) within the heme pocket of *Cb*-SONO induced by the activator BAY 41-2272. (a) Transient absorption spectra of the heme Soret band at selected time delays showing that CO binding to the heme is being probed. (b) Comparison of CO dynamics up to 5 ns for sGC and *Cb*-SONO in the absence and presence of the BAY 41-2272. All kinetics were fitted to a multiexponential function whose parameters are listed in Table 1.

In the presence of CO bound to the heme, a 3.5-nm shift of Soret band is induced by BAY 41-2272 binding to sGC-CO (Figure 2a), and a 1-nm shift is observed in the case of *Cb*-SONO (Figure 2c). The shift of the Soret band was systematically observed with various preparations of sGC and also in the presence of the activator YC-1 (Supporting Figure

S1). The simultaneous presence of the nonhydrolyzable substrate analogue GTP-γ-S induces an even larger blue-shift of the Soret (Supporting Figure S1), indicating a larger conformational change of sGC. The α- and β-bands are also affected by the binding of CO: a 4-nm down-shift affects the β-band in sGC spectrum with a broadening of the α-band. For

Table 1. Parameters of Global Fit of the CO Binding Kinetics (Figure 4) to a Multiexponential Function[a]

protein	τ_1 (A_1)	τ_2 (A_2)	τ_3 (A_3)	τ_4 (A_4)	τ_5 (A_5)	τ_6 (A_6)
Cb SONO	7 ps (0.05)	100 ps (0.03)	8 ns (0.08)			0.5 ms (0.84)
Cb SONO +BAY	7 ps (0.05)	80 ps (0.06)	3.5 ns (0.21)		6 μs (0.05)	0.7 ms (0.63)
sGC	6 ps (0.07)	120 ps (0.01)	5.7 ns (0.05)	0.9 μs (0.02)	0.1 ms (0.06)	10 ms (0.79)
sGC +BAY +GTP-γ-S	6 ps (0.09)	90 ps (0.20)	1.2 ns (0.13)	16 ns (0.10)	12 μs (0.08) 0.4 ms (0.16)	6 ms (0.22)
β_1(200)	18 ps (0.17)	190 ps (0.22)	0.95 ns (0.16)	35 ns (0.05)	0.1 ms (0.25)	1.6 ms (0.15)
β_1(200) +BAY	10 ps (0.18)	100 ps (0.22)	0.8 ns (0.17)	19 ns (0.11)	5 μs (0.14) 76 μs (0.10)	0.6 ms (0.08)

[a]Time constants (τ_i) are given with their relative amplitudes A_i such that $\Sigma A_i = 1$.

Cb-SONO, the α-band shifts by 0.5 nm upon the binding of BAY 41-2272 to Cb-SONO-CO. It should be noted that the effect induced by BAY 41-2272 on the spectrum of Cb-SONO is mostly observed in the absence of CO, while it is conspicuous for sGC in the presence of CO. This point will be discussed below.

These shifts show that the binding of BAY 41-2272 influences the electronic molecular orbitals of the heme, an effect that stems from modified structural constraints and heme distortion due to a conformational change induced by the activator. In the case of Cb-SONO, the binding of BAY 41-2272 necessarily occurs to the heme domain, and this leads to the hypothesis that it does so to sGC. We thus compared the effect of BAY 41-2272 on ligand dynamics in both proteins with that in the isolated heme domain β_1(200) from sGC.

Ligand Dynamics Induced by the Activator BAY 41-2272. Because BAY 41-2272 and CO activate sGC[15,16] in synergy, we studied the dynamics of the interaction between CO and both sGC and Cb-SONO to probe the effects induced by the effector. We measured CO rebinding during the first 5 ns following its dissociation from the heme (Figure 3) with a 1-ps time resolution in order to measure the exact contribution of the fast rebinding phases. The CO geminate rebinding to Cb-SONO is identified by the probed transient spectra of the process (Figure 3a), which are identical to the steady-state spectral difference [unliganded *minus* CO-liganded Cb-SONO]. The substates of CO dissociated and moving in different sites within the protein have the same electronic spectrum but are distinguished by their time constants due to different energy barriers to be overcome from one state to the other. Because these energy barriers depend upon the structure, the modulation of time constants and their amplitude translates conformational changes in the protein.

In the 5-ns time range, CO moves within the heme pocket and rebinds from the heme pocket. The kinetics (Figure 3b), representing the evolution of the entire spectra, show that this geminate rebinding of CO occurs only modestly to native sGC and Cb-SONO. Remarkably, this process is strongly enhanced in the presence of BAY 41-2272, and this enhancement is similar in both proteins (fitted kinetic parameters in Table 1). We have verified that DMSO alone does not alter the electronic spectrum or the kinetics of CO rebinding to Cb-SONO (Supporting Figure S2). This fast CO rebinding occurs even more quickly for sGC in the presence of the substrate analogue GTP-γ-S (Cb-SONO does not have a GTP binding site) and is multiphasic, similar to NO dynamics in the enzyme NO-synthase.[41] GTP-γ-S has additional effects on the conformation of sGC (Supporting Figure S1) and drives it further toward the activated state. To obtain a measurement of CO dynamics with sGC in a conformation as close as possible to the fully activated

state, which is the real one in the presence of GTP and NO, the next measurement of sGC-CO dynamics was carried out in the presence of GTP-γ-S bound to sGC.

In order to obtain a complete overview of the structural effects induced by BAY 41-2272 on the CO-heme sensor interaction by measuring all the transitions, we aimed at comparing the CO dynamics for both proteins (Figure 4) in the unusually broad time range encompassing 12 orders of magnitude (from 0.5 ps to 0.3 s). Indeed, CO dynamics within the heme pocket or the protein core (geminate rebinding) are probed in the ps–ns (and partly μs) time range, whereas bimolecular rebinding from solvent is probed in the ms (and partly μs) time range. Thus, the comparison of kinetics in Figure 4 provides a wealth of information. First, one remarks that all six kinetics comprise a plateau between ~0.1–1 μs that separates fast geminate rebinding phases and slower bimolecular rebinding phases. Second, for both geminate and bimolecular phases, different behaviors between the proteins are clearly revealed by visual examination of the kinetics. We fitted the data in the entire time range to a multiexponential function; the kinetic parameters of the global fit (time constants τ_i and their relative amplitudes A_i) are given in Table 1, and the mechanistic significance of all rebinding phases are given in Figure 5.

The CO dynamics appear multiphasic throughout the entire time range, revealing multiple energy barriers for CO rebinding. The observed phases are assigned to the dynamics of CO in the heme pocket[36,37] (τ_1 and τ_2), CO in docking sites[39] (τ_3 and τ_4), and bimolecular rebinding (diffusion) from solvent[40] (τ_5 and τ_6) as depicted in Figure 5. For both Cb-SONO (Figure 4a) and full-length sGC (Figure 4b) the second and third components (τ_2 and τ_3) are faster and have a larger amplitude in the presence of BAY 41-2272. This is remarkable and demonstrates that both proteins react in exactly the same manner as the binding of BAY 41-2272. Since this effect is observed for CO dynamics in the ps–ns time range, we conclude that the same conformational change occurred in the heme pocket of these two homologous proteins. As for the heme domain β_1(200), we also found a faster CO rebinding in the presence of BAY 41-2272 (Figure 4c) with a decrease of all three time constants but with a lower amplitude (Table 1). This shows that in the absence of the activator, CO geminate rebinding to the isolated heme domain is predominant and already as fast as in sGC in the presence of the activator. This observation is important and will be further discussed below with respect to allostery.

The fastest time constant $\tau_1 = 6$–7 ps is identical to that measured for NO rebinding to the 4-coordinate heme after dissociation of 5c-NO heme,[36,37,42] suggesting the involvement of a 5-coordinate heme-CO (Fe-His bond cleaved) in the
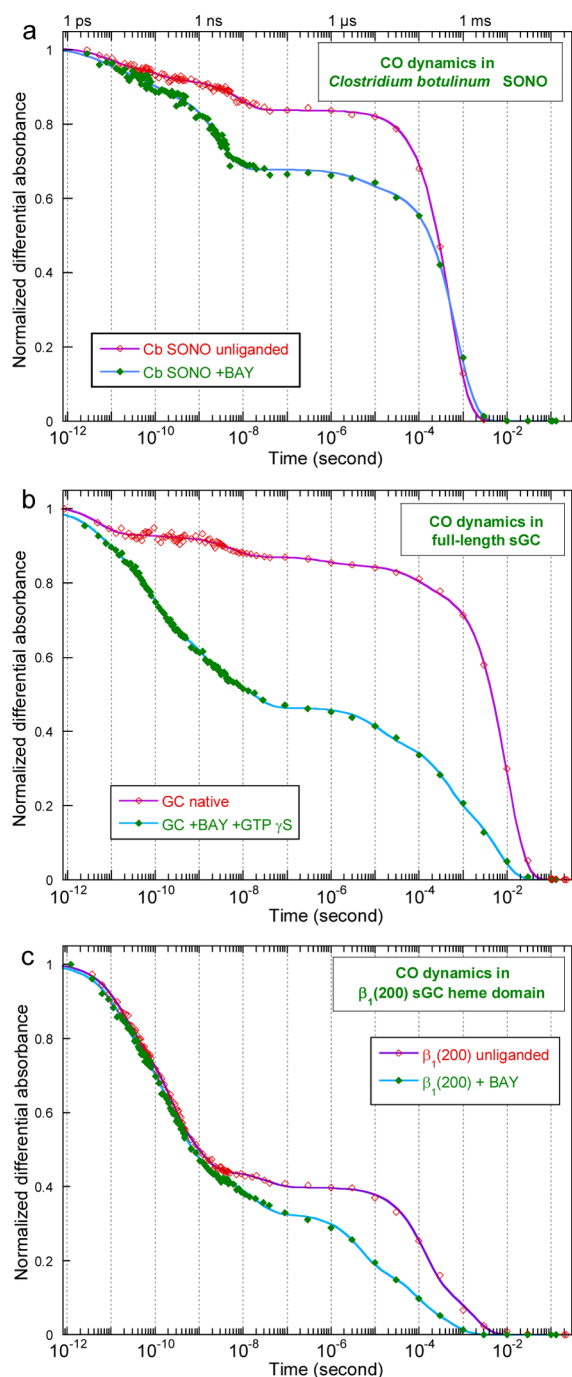
Figure 4. Dynamics of CO interacting with the heme in a broad time range from 0.5 ps to 0.3 s both in the absence (red symbols) and in the presence of the activator BAY 41-2272 (green symbols): (a) in Cb SONO; (b) in full-length sGC; (c) in the isolated heme domain $\beta_1(200)$. All kinetics were fitted to a multiexponential function whose parameters are listed in Table 1.

synergistic activation of sGC. Similarly with the well-studied myoglobin case,[39] the intermediate time constant τ_4 in the time interval 0.1−1 μs is assigned to CO rebinding from a "docking site" in the protein core. This phase is not present in the case of Cb-SONO but only in sGC and its isolated domain $\beta_1(200)$ with small amplitudes (0.02 and 0.05, respectively). Remarkably, the presence of BAY 41-2272 increases this amplitude (0.10 and 0.11) and decreases the time constant to values similar for sGC (τ_4 = 16 ns) and for $\beta_1(200)$ (19 ns); this

component was also detected (17 ns) in a limited linear time-range for sGC from *Manduca sexta*.[43] The fact that BAY 41-2272 induces the same effect on CO internal dynamics in sGC and its isolated heme domain $\beta_1(200)$ indicates that the same structural transition occurred in both cases, and consequently that the effector binds to the 1−200 domain in full-length sGC.

On the other side of the time scale, the time constant of bimolecular rebinding of CO from the solution depends upon CO concentration[40,44] and can occur with a time constant as fast as 1 μs with $[CO]$ = 1 mM.[40] This bimolecular rebinding occurs with time constants of 0.5 and 10 ms for Cb-SONO and full-length sGC respectively, yielding association rates constants k_{on} = 1.5 × 10^6 M^{-1} s^{-1} for Cb-SONO and k_{on} = 0.75 × 10^5 M^{-1} s^{-1} for sGC (Table 2). Thus, CO binding to Cb-SONO from solution appears faster than to sGC. Now, in the presence of BAY 41-2272, the relative amplitude of bimolecular rebinding decreases for Cb-SONO (as a consequence of more efficient geminate rebinding), yet it occurs with the same time constant. This is at variance with the case of full-length sGC where not only did the amplitude decrease, but so did all the time constants of the multiphasic CO rebinding dynamics, including bimolecular (CO from the solvent) and geminate (CO still in the heme pocket). Because BAY 41-2272 modifies all the time constants of CO dynamics in sGC, we readily conclude that this effector induces a major conformational change not only in the heme pocket but also extended to the entire protein. As a result of this conformational change, the CO association rate from solution is much higher and almost diffusion-limited (k_{on} = 1.25 × 10^8 and 0.75 × 10^8 M^{-1} s^{-1} in the presence of BAY 41-2272 for Cb-SONO and sGC, respectively). In Cb-SONO, homologous but limited to the heme domain of dimeric sGC, we observed the same structural changes upon binding of the effector as in sGC, yet those effects on time constants are limited to the ps−ns range, reflecting changes in dynamics and energy barriers within the heme pocket. In other words, CO association to Cb-SONO from solvent is fast because of the absence of any other β-domain and α-subunit. The fact that the rate of CO bimolecular rebinding to Cb-SONO is not changed by BAY 41-2272 but is modified in the full-length sGC shows that the conformational change induced by BAY 41-2272 involved both subunits of sGC.

Isolated $\beta_1(200)$ Heme Domain. Similarly as with full-length sGC, the bimolecular rebinding of CO appears biphasic. Such a biphasic process has been observed in the case of tetrameric human hemoglobin A (HbA)[40] and was assigned to the interconversion of R to T states in the same time scale as ligand rebinding. For an isolated subunit, the biphasic character of bimolecular rebinding may come from the fluctuating position of a side-chain involved in the accessibility of the heme pocket, as was observed in the case of HbA in which the gating His was mutated to Trp, which fluctuates between blocked and open positions.[40]

For the isolated heme domain $\beta_1(200)$ the time constant of bimolecular rebinding (k_{on} = 0.47 × 10^6 M^{-1} s^{-1}) is faster than for sGC but similar to that of Cb-SONO. Thus, because Cb-SONO and $\beta_1(200)$ have the same length and folding, this similarity leads one to attribute the difference of k_{on} between sGC and Cb-SONO to higher accessibility of the heme to CO in Cb-SONO than in full-length sGC because of the presence of additional β-domains and α-subunit. On the other hand, the overall CO dynamics for $\beta_1(200)$ in absence of BAY 41-2272 through the 12-decade time range is very similar to that
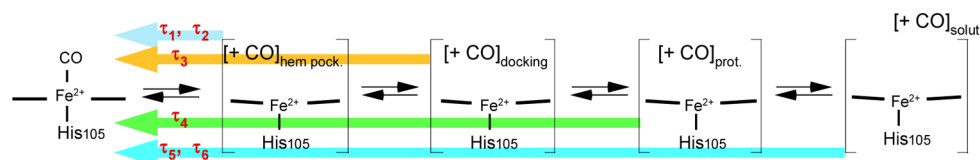
Figure 5. Correspondence between the measured time constants and the rebinding of CO to the heme from different states of the protein–ligand system. The subscripts indicate the different positions of CO with respect to the protein: in the heme pocket, docking site, protein core, and in solvent, respectively. τ_1 and τ_2 correspond to two positions of CO within the heme pocket, whereas τ_5 and τ_6 correspond to two different conformations of the protein or at least of the entry channel. Contrary to CO in solvent, the other phases involve the same CO molecule that was photodissociated.

Table 2. CO Association Rates Calculated from Bimolecular Rebinding Time Constants (τ_5 and τ_6) with $[CO]$ = 1.33 mM[a]

protein	k_{on} (M^{-1} s^{-1}) (fast phase)	k_{on} (M^{-1} s^{-1}) (slow phase)
Cb SONO		$(1.5 \pm 0.1) \times 10^6$
Cb SONO +BAY	$(1.25 \pm 0.5) \times 10^8$	$(1.07 \pm 0.1) \times 10^6$
sGC	$(0.75 \pm 0.2) \times 10^7$	$(0.75 \pm 0.1) \times 10^5$
sGC +BAY +GTP-γ-S	$(0.8 \pm 0.2) \times 10^8$	$(1.25 \pm 0.3) \times 10^5$
	$(1.9 \pm 0.3) \times 10^6$	
$\beta_1(200)$	$(0.75 \pm 0.1) \times 10^7$	$(0.47 \pm 0.1) \times 10^6$
$\beta_1(200)$ +BAY	$(1.5 \pm 0.5) \times 10^8$	$(1.25 \pm 0.2) \times 10^6$
	$(1 \pm 0.2) \times 10^7$	

[a]The amplitudes are same as A_5 and A_6 in Table 1.

observed with the full-length sGC in the presence of BAY 41-2272. This means that $\beta_1(200)$ adopts a structural conformation that is very close to that of the activated state of sGC (i.e., with BAY 41-2272 or NO bound to the heme). The corresponding kinetic parameters (Table 1) are as follows: BAY 41-2272 induces CO rebinding phases in sGC (τ_3 = 1.2 ns, τ_4 = 16 ns for CO motion from internal docking sites, and τ_5 = 0.4 ms for CO diffusing from solvent) that are similar (in time constants as well as in amplitudes) to those occurring in $\beta_1(200)$ in the absence of the effector (τ_3 = 0.95 ns, τ_4 = 35 ns, and τ_5 = 0.1 ms). Consequently, we conclude that BAY 41-2272 induces a conformation of sGC similar to that of the isolated heme domain in the absence of effector (since Cb-SONO and $\beta_1(200)$ are monomers, the binding of BAY 41-2272 cannot have full allosteric effects *stricto sensu* conveyed to a catalytic site, but the change in CO dynamics proves that structural changes occurred, similarly as with those present in sGC).

Allostery in sGC. The present observations support a previous hypothesis:[38] in the absence of the α-subunit and of the remaining part of β-subunit, the isolated heme domain $\beta_1(200)$ adopts an activated conformation. This agrees with a slower relaxation of the isolated $\beta_1(385)$ fragment in comparison with full-length sGC observed by transient Raman spectroscopy after CO photolysis.[45] The effect of BAY 41-2272 on Cb-SONO in the ps–ns time range seems larger because Cb-SONO does not adopt the relaxed conformation of isolated $\beta_1(200)$. Its effect on isolated heme $\beta_1(200)$ is to drive the structure more completely toward the activated state, as deduced from the faster dynamics in the nanosecond to millisecond phases and slightly faster picosecond phases when the effector is bound (Figure 4c and Table 1). This effect is a clear consequence of the interaction between subunits since the structural constraints on $\beta_1(200)$ are decreased by the lack of the α-subunit and $\beta_1(201-619)$ domain, so that $\beta_1(200)$ adopts a more relaxed conformation.

This constitutes a direct demonstration of allostery in sGC. A similar observation is made for isolated HbA subunits, which adopt a relaxed R-state conformation, because of the absence of intersubunit constraints existing in the tetramer.[40]

The overall picture is that binding of the allosteric effector triggers a conformational change, not only localized in the heme pocket but also in the entire heme domain, which is then transmitted to the catalytic site of sGC through interactions between both subunits. In absence of these interactions, the isolated heme domain relaxes to the activated state without effector, whose binding further shifts the energy minimum of the molecule to the activated conformation.

Relation with Previous Experiments. Our results unambiguously demonstrate that BAY 41-2272 binds to the domain 1–200 of sGC and Cb-SONO and that this binding is sufficient to trigger a structural transition in both proteins. Importantly, Cb-SONO has partly the behavior of sGC and partly that of the isolated $\beta_1(200)$ heme domain. We infer that the sGC heme domain contains all the structural features necessary for the CO/BAY synergistic activation. So far, various and contradictory results have been reported about the localization of the sGC activators binding site. Previous experiments[26–30] aimed at localizing the YC1 or BAY 41-2272 binding site with mutations either in the α-subunit[26,29] or in the β-subunit[26,29,46] identified residues involved in sGC activation induced by NO or by activators. Several locations were speculated for this site, including the "pseudosymmetric" site[26] and the H-NOX pocket in α-subunit.[27] However, measuring the activity of mutated sGC does not discriminate between the role of side-chains in activation or in binding activators and does not permit to localize the activator site. Competition binding measurements showed that the BAY 41-2272 site can also bind some nucleotides,[47] but this fact does not imply that it corresponds necessarily the to "pseudosymmetric" site.

Whereas the effect of YC1 and BAY 41-2272 on full-length sGC was detected by EPR spectroscopy,[31] no effect was observed on β_2-(217)-NO or β_1-(385)-NO heme domain constructs.[31] Possibly these nitrosylated constructs are in a fully activated conformation so that EPR cannot detect further changes in structure due the activators, whereas the dynamics of CO is sensitive to subtle changes far from the heme. The observation that a photoactivable derivative of BAY 41-2272 has labeled side-chains of α-subunit[12] (Cys238 and Cys243) does not contradict our results: in that case, the bulky photolabeling moiety linked to the activator derivative very likely interacts with side-chains more distant and not directly involved in the BAY 41-2272 binding site. Finally, our result agrees with changes induced by the cognate compound YC-1 in Raman spectra of the sGC domain $\beta_1(385)$[24,48] or of the full-length sGC.[19,34]

Summary and Conclusions. In summary, we have demonstrated that the regulatory site where BAY 41-2272 binds resides in the portion $\beta(1-200)$ of the sGC heme domain. Binding of the activator to this domain is sufficient to trigger a conformational change toward the sGC activated state, which controls the dynamics of CO. We also showed that BAY 41-2272 binds to the NO-sensor of the bacteria *C. botulinum*, which is coupled to a protein domain homologous to the methyl-accepting chemotaxis protein. In recent years, numerous SONO proteins were discovered in bacteria. The SONO (H-NOX) proteins from two bacteria of the genus *Vibrio* have been recently shown to be involved in quorum sensing through the detection of NO.[49,50] Two other SONO (from *Legionella* and *Shewanella*) are involved in regulation of cyclic-di-GMP synthesis in a NO-dependent manner so that the NO-liganded SONO restricts the biofilm formation.[51,52] Thus, cognate compounds of BAY 41-2272 could exert a control on the behavior of particular bacteria (including *C. botulinum*) with respect to their response to the presence of NO or NO-donors.

METHODS

Preparation of the Full-Length Soluble Guanylate Cyclase. sGC was purified from bovine lung by chromatography, and its activity was assayed as previously described.[36] sGC was obtained directly in the ferrous state after the last column ($\lambda_{max} = 431$ nm). The final buffer was triethanolamine 25 mM, NaCl 50 mM, DTT 1 mM, MgCl$_2$ 1 mM, pH 7.4. An aliquot of sGC in buffer ($70-100$ μL at ~ 20 μM) was put in a quartz cell (1-mm optical path length) sealed with a rubber stopper and degassed with four cycles of vacuuming and purging with argon (Air Liquide, 99.999%) so that O$_2$ was completely removed. For preparing CO-liganded sGC, 100% CO gas phase at 1.3 bar (0.13 MPa) was directly introduced in the vacuumed spectroscopic cell through the gas train, yielding 1.33 mM of CO in the aqueous phase. Full equilibration was obtained by waiting 30 min with the cell still connected to the gas train, ensuring an "infinite" reservoir of CO. Then, a second stopper in silicone, with vacuum grease, was stacked on the cell. Steady-state absorption spectra (Shimadzu 1700 spectrophotometer) were recorded for monitoring the evolution of CO binding, and after the laser measurements to verify the state of the sample. The absorbance of the CO-liganded sGC was in the range 0.2–0.3 for 1 mm at the maximum of the Soret band.

To prepare the proteins liganded with the activator BAY 41-2272, we first prepared a stock solution of activator in DMSO (dimethylsulfoxide) and added 5 μL directly in the spectroscopic cell to obtain a final concentration of 200 μM, necessary to ensure the saturation of 20 μM sGC. The samples were incubated for 2 h at 4 °C in the presence of activator in the dark. To prepare sGC liganded with the subtrate analogue GTP-γ-S, we first prepared a stock solution in buffer and added 10 μL in the spectroscopic cell to obtain a final concentration of 1 mM. BAY 41-2272 was purchased from Alexis. GTP-γ-S were purchased from Sigma Chemicals.

Preparation of Bacterial SONO and the Heme Domain $\beta_1(200)$ of Human Soluble Guanylate Cyclase. The isolated domain $\beta_1(200)$ has a sequence strictly identical for both human and bovine species. The expression and purification of isolated heme domain $\beta_1(200)$ of human sGC and of bacterial SONO(186) from *C. botulinum* was performed as previously described.[17] The final buffer was 50 mM triethanolamine, 300 mM NaCl, 5% (v/v) glycerol, pH 8.2. The SONO and the isolated heme domain were prepared for spectroscopy similarly as sGC, except for a supplementary step of reduction: after vacuuming, a 10-μL aliquot of sodium dithionite (5 mM) was introduced into the cell with a gastight syringe to obtain final concentration of 0.5 mM. The reduction of the heme was monitored by measuring the spectrum before adding 100% CO. The absorbance of the CO-liganded SONO was in the range 0.4–0.6 for 1 mm at the maximum of the Soret band.

Femtosecond to Picosecond Time-Resolved Absorption Spectroscopy. Transient spectra were recorded simultaneously with kinetics as a time-wavelength matrix data using the pump–probe laser system previously described.[53] Photodissociation of CO was achieved by excitation in the Q-bands of the heme ($\lambda_{ex} = 564$ nm; pulse duration $\Delta t \approx 40$ fs; repetition rate 30 Hz). The entire transient absorption spectrum after a variable delay between dissociating and probe pulses was recorded with a CCD detector. The global analysis of the data was performed by singular value decomposition (SVD) of the time-wavelength matrix as described.[53] The SVD component having the highest singular value corresponded to the geminate rebinding, and its kinetics were fit to a minimum number of exponential components. The absorption kinetics represent the evolution of the difference spectrum, taking into account both the 5-coordinate deoxy heme decay and the appearance of the 6-coordinate CO-liganded heme. The time constants were obtained from fitting the average of several scans (up to 24).

Nanosecond to Second Time-Resolved Absorption Spectroscopy. To measure the nanosecond geminate and bimolecular CO rebindings, we have used a home-built spectrophotometer with an extended time-range for detection, from 5 ns to 1 s, based on two lasers that are electronically synchronized.[54] The photodissociating pulse (pulse duration $\Delta t \approx 5$ ns) is tuned at 532 nm in the Q-band of the heme. The probing pulse, provided by a tunable optical parametric oscillator, is tuned at 450 nm to probe the kinetics of differential absorption due to the disappearance of 5-coordinate dissociated heme. The electronic time delay after the dissociating pulse was changed linearly from 1 to 30 ns and then was changed with a half-log$_{10}$ progression from 30 ns to 0.3 s. Eight scans were averaged for each kinetics. Importantly, the same samples were used for the picosecond and for the nanosecond to second measurements. Because the kinetics in the ps–ns time range ended at 5 ns and the kinetics in the ns–s time range started at 1 ns, there is a temporal overlap from 1 to 5 ns that allows the merging of both measurements, provided that the same sample is used for both time ranges.

ASSOCIATED CONTENT

Ⓢ Supporting Information

This material is available free of charge *via* the Internet at http://pubs.acs.org.

AUTHOR INFORMATION

Corresponding Author
*E-mail: michel.negrerie@polytechnique.fr.

Notes
The authors declare no competing financial interest.

ACKNOWLEDGMENTS

ABBREVIATIONS

cGMP, cyclic guanosine monophosphate; sGC, soluble guanylate cyclase; SONO, sensor of nitric oxide; $\beta_1(200)$, heme domain of sGC restricted to the 200 first residues; H-NOX, heme-nitric oxide and oxygen binding domain

REFERENCES

(1) Ignarro, L. J., Buga, G. M., Wood, K. S., Byrns, R. E., and Chaudhuri, G. (1987) Endothelium-derived relaxing factor produced and released from artery and vein is nitric oxide. *Proc. Natl. Acad. Sci. U.S.A. 84*, 9265–9269.

(2) Palmer, R. M. J., Ferrige, A. G., and Moncada, S. (1987) Nitric oxide release accounts for the biological activity of endothelium-derived relaxing factor. *Nature 327*, 524−526.

(3) Bian, K., Doursout, M. F., and Murad, F. (2008) Vascular system: role of nitric oxide in cardiovascular diseases. *J. Clin. Hypertens. 10*, 304−310.

(4) Coggins, M. P., and Bloch, K. D. (2007) Nitric oxide in the pulmonary vasculature. *Arterioscler. Thromb. Vasc. Biol. 27*, 1877−1885.

(5) Nagy, G., Clark, J. M., Buzas, E. I., Gorman, C. L., and Cope, A. P. (2007) Nitric oxide, chronic inflammation and autoimmunity. *Immunol. Lett. 111*, 1−5.

(6) Blaise, G. A., Gauvin, D., Gangal, M., and Authier, S. (2005) Nitric oxide, cell signaling and cell death. *Toxicology 208*, 177−192.

(7) Evgenov, O. V., Pacher, P., Schmidt, P. M., Hasko, G., Schmidt, H. H. W., and Stasch, J.-P. (2006) NO-independent stimulators and activators of soluble guanylate cyclase: discovery and therapeutic potential. *Nat. Rev. Drug Discovery 5*, 755−768.

(8) Mittendorf, J., Weigand, S., Alonso-Alija, C., Bischoff, E., Feurer, A., Gerisch, M., Kern, A., Knorr, A., Lang, D., Muenter, K., Radtke, M., Schirok, H., Schlemmer, K.-H., Stahl, E., Straub, A., Wunder, F., and Stasch, J.-P. (2009) Discovery of riociguat (BAY 63−2521): a potent, oral stimulator of soluble guanylate cyclase for the treatment of pulmonary hypertension. *Chem. Med. Chem. 4*, 853−865.

(9) Miller, L. N., Nakane, M., Hsieh, G. C., Chang, R. J., Kolasa, T., Moreland, R. B., and Brioni, J. D. (2003) A-350619: a novel activator of soluble guanylate cyclase. *Life Sci. 72*, 1015−1025.

(10) Ko, F. N., Wu, C. C., Kuo, S. C., Lee, F. Y., and Teng, C. M. (1994) YC-1, a novel activator of platelet guanylate cyclase. *Blood 84*, 4226−4233.

(11) Stasch, J. P., Pacher, P., and Evgenov, O. V. (2011) Soluble guanylate cyclase as an emerging therapeutic target in cardiopulmonary disease. *Circulation 123*, 2263−2273.

(12) Stasch, J. P., Becker, E. M., Alonso-Alija, C., Apeler, H., Dembowsky, K., Feurer, A., Gerzer, R., Minuth, T., Perzborn, E., Pleiss, U., Schroder, H., Schroeder, W., Stahl, E., Steinke, W., Straub, A., and Schramm, M. (2001) NO-independent regulatory site on soluble guanylate cyclase. *Nature 410*, 212−215.

(13) Galle, J., Zabel, U., Hubner, U., Hatzelmann, A., Wagner, B., Wanner, C., and Schmidt, H. H. W. (1999) Effects of the soluble guanylyl cyclase activator, YC-1, on vascular tone, cyclic GMP levels and phosphodiesterase activity. *Br. J. Pharmacol. 127*, 195−203.

(14) Mülsch, A., Bauersachs, J., Schafer, A., Stasch, J. P., Kast, R., and Busse, R. (1997) Effect of YC-1, an NO-independent, superoxide-sensitive stimulator of soluble guanylyl cyclase, on smooth muscle responsiveness to nitrovasodilators. *Br. J. Pharmacol. 120*, 681−689.

(15) Friebe, A., Schultz, G., and Koesling, D. (1996) Sensitizing soluble guanylyl cyclase to become a highly CO-sensitive enzyme. *EMBO J. 15*, 6863−6868.

(16) Stone, J. R., and Marletta, M. A. (1998) Synergistic activation of soluble guanylate cyclase by YC-1 and carbon monoxide: implications for the role of cleavage of the iron-histidine bond during activation by nitric oxide. *Chem. Biol. 5*, 255−261.

(17) Nioche, P., Berka, V., Vipond, J., Minton, N., Tsai, A.-L., and Raman, C. S. (2004) Femtomolar sensitivity of a NO sensor from Clostridium botulinum. *Science 306*, 1550−1553.

(18) Pellicena, P., Karow, D. S., Boon, E. M., Marletta, M. A., and Kuriyan, J. (2004) Crystal structure of an oxygen-binding heme domain related to soluble guanylate cyclases. *Proc. Natl. Acad. Sci. U.S.A. 101*, 12854−12859.

(19) Pal, B., and Kitagawa, T. (2005) Interactions of soluble guanylate cyclase with diatomics as probed by resonance Raman spectroscopy. *J. Inorg. Chem. 99*, 267−279.

(20) Poulos, T. L. (2006) Soluble guanylate cyclase. *Curr. Opin. Struct. Biol. 16*, 736−743.

(21) Winger, J. A., Derbyshire, E. R., and Marletta, M. A. (2007) Dissociation of nitric oxide from soluble guanylate cyclase and heme-nitric oxide/oxygen binding domain constructs. *J. Biol. Chem. 282*, 897−907.

(22) Derbyshire, E. R., and Marletta, M. A. (2007) Butyl isocyanide as a probe of the activation mechanism of soluble guanylate cyclase. *J. Biol. Chem. 282*, 35741−35748.

(23) Ma, X., Sayed, N., Beuve, A., and van den Akker, F. (2007) NO and CO differentially activate soluble guanylyl cyclase via a heme pivot-bend mechanism. *EMBO J. 26*, 578−588.

(24) Denninger, J. W., Schelvis, J. P. M., Brandish, P. E., Zhao, Y., Babcock, G. T., and Marletta, M. A. (2000) Interaction of soluble guanylate cyclase with YC-1: Kinetic and resonance Raman studies. *Biochemistry 39*, 4191−4198.

(25) Russwurm, M., Mergia, E., Mullershausen, F., and Koesling, D. (2002) Inhibition of deactivation of NO-sensitive guanylyl cyclase accounts for the sensitizing effect of YC-1. *J. Biol. Chem. 277*, 24883−24888.

(26) Lamothe, M., Chang, F. J., Balashova, N., Shirokov, R., and Beuve, A. (2004) Functional characterization of nitric oxide and YC-1 activation of soluble guanylyl cyclase: Structural implication for the YC-1 binding site? *Biochemistry 43*, 3039−3048.

(27) Hu, X. H., Murata, L. B., Weichsel, A., Brailey, J. L., Roberts, Sue A., Nighorn, A., and Montfort, W. R. (2008) Allostery in recombinant soluble guanylyl cyclase from *Manduca sexta*. *J. Biol. Chem. 283*, 20968−20977.

(28) Pal, B., and Kitagawa, T. (2010) Binding of YC-1/BAY 41-2272 to soluble guanylate cyclase: a new perspective to the mechanism of action. *Biochem. Biophys. Res. Commun. 397*, 375−379.

(29) Friebe, A., Russwurm, M., Mergia, E., and Koesling, D. (1999) A point-mutated guanylyl cyclase with features of the YC-1 stimulated enzyme: implications for the YC-1 binding site? *Biochemistry 38*, 15253−15257.

(30) Koglin, M., and Behrends, S. (2003) A functional domain of the α_1 subunit of soluble guanylate cyclase is necessary for activation of the enzyme by nitric oxide and YC-1 but is not involved in heme binding. *J. Biol. Chem. 278*, 12590−12597.

(31) Derbyshire, E. R., Gunn, A., Ibrahim, M., Spiro, T. G., Britt, R. D., and Marletta, M. A. (2008) Characterization of two different five-coordinate soluble guanylate cyclase ferrous-nitrosyl complexes. *Biochemistry 47*, 3892−3899.

(32) Pal, B., Li, Z. Q., Ohta, T., Takenaka, S., Tsuyama, S., and Kitagawa, T. (2004) Resonance Raman study on synergistic activation of soluble guanylate cyclase by imidazole, YC-1 and GTP. *J. Inorg. Chem. 98*, 824−832.

(33) Li, Z., Pal, B., Takenaka, S., Tsuyama, S., and Kitagawa, T. (2005) Resonance Raman evidence for the presence of two heme pocket conformations with varied activities in CO-bound bovine soluble guanylate cyclase and their conversion. *Biochemistry 44*, 939−946.

(34) Makino, R., Obayashi, E., Homma, N., Shiro, Y., and Hori, H. (2003) YC-1 facilitates release of the proximal his residue in the NO and CO complexes of soluble guanylate cyclase. *J. Biol. Chem. 278*, 11130−11137.

(35) Martin, E., Czarnecki, K., Jarayaman, V., Murad, F., and Kincaid, J. (2005) Resonance Raman and infrared spectroscopic studies of high-output forms of human soluble guanylyl cyclase. *J. Am. Chem. Soc. 127*, 4625−4631.

(36) Negrerie, M., Bouzhir, L., Martin, J. L., and Liebl, U. (2001) Control of nitric oxide dynamics by guanylate cyclase in its activated state. *J. Biol. Chem. 276*, 46815−46821.

(37) Negrerie, M., Kruglik, S. G., Lambry, J.-C., Vos, M. H., Martin, J.-L., and Franzen, S. (2006) Role of heme iron coordination and protein structure in the dynamics and geminate rebinding of nitric oxide to H93G myoglobin: Implications for NO-sensors. *J. Biol. Chem. 281*, 10389−10398.

(38) Yoo, B. K., Lamarre, I., Martin, J. L., and Negrerie, M. (2012) Quaternary structure controls ligand dynamics in soluble guanylate cyclase. *J. Biol. Chem. 287*, 6851−6859.

(39) Olson, J. S., Soman, J., and Phillips, G. N. (2007) Ligand pathways in myoglobin: a review of Trp cavity mutations. *IUBMB Life 59*, 552−562.

(40) Birukou, I., Soman, J., and Olson, J. S. (2011) Blocking the gate to ligand entry in human hemoglobin. *J. Biol. Chem. 286*, 10515−10529.

(41) Gautier, C., Negrerie, M., Wang, Z.-Q., Lambry, J.-C., Stuehr, D. J., Collin, F., Martin, J.-L., and Slama-Schwok, A. (2004) Dynamic regulation of the inducible nitric-oxide synthase by NO: comparaison with the endothelial isoform. *J. Biol. Chem. 279*, 4358−4365.

(42) Kruglik, S. G., Lambry, J.-C., Cianetti, S., Martin, J.-L., Eady, R. R., Andrew, C. R., and Negrerie, M. (2007) Molecular basis for nitric oxide dynamics and affinity with *Alcaligenes xylosoxidans* cytochrome *c′*. *J. Biol. Chem. 282*, 5053−5062.

(43) Hu, X., Feng, C. J., Hazzard, J. T., Tollin, G., and Montfort, W. R. (2008) Binding of YC-1 or BAY 41-2272 to soluble guanylyl cyclase induces a geminate phase in CO photolysis. *J. Am. Chem. Soc. 130*, 15748−15749.

(44) Sharma, V. S., Magde, D., Kharitonov, V. G., and Koesling, D. (1999) Soluble guanylate cyclase: effect of YC-1 on ligation kinetics with carbon monoxide. *Biochem. Biophys. Res. Commun. 254*, 188−191.

(45) Schelvis, J. P. M., Kim, S., Zhao, Y., Marletta, M. A., and Babcock, G. T. (1999) Structural dynamics in the guanylate cyclase heme pocket after CO photolysis. *J. Am. Chem. Soc. 121*, 7397−7400.

(46) Rothkegel, C., Schmidt, P. M., Stoll, F., Schröder, H., Schmidt, H. H. W., and Stasch, J.-P. (2006) Identification of residues crucially involved in soluble guanylate cyclase activation. *FEBS Lett. 580*, 4205−4213.

(47) Yazawa, S., Tsuchiya, H., Hori, H., and Makino, R. (2006) Functional characterization of two nucleotide-binding sites in soluble guanylate cyclase. *J. Biol. Chem. 281*, 21763−21770.

(48) Ibrahim, M., Derbyshire, E. R., Marletta, M. A., and Spiro, T. G. (2010) Probing soluble guanylate cyclase activation by CO and YC-1 using resonance Raman spectroscopy. *Biochemistry 49*, 3815−3823.

(49) Wang, Y., Dufour, Y. S., Carlson, H. K., Donohue, T. J., Marletta, M. A., and Ruby, E. G. (2010) H-NOX−mediated nitric oxide sensing modulates symbiotic colonization by *Vibrio fischeri*. *Proc. Natl. Acad. Sci. U.S.A. 107*, 8375−8380.

(50) Henares, B. M., Higgins, K. E., and Boon, E. M. (2012) Discovery of a nitric oxide responsive quorum sensing circuit in *Vibrio harveyi*. *ACS Chem. Biol. 7*, 1331−1336.

(51) Carlson, H. K., Vance, R. E., and Marletta, M. A. (2010) HNOX regulation of c-di-GMP metabolism and biofilm formation in *Legionella pneumophila*. *Mol. Microbiol. 77*, 930−942.

(52) Liu, N., Xu, Y., Hossain, S., Huang, N., Coursolle, D., Gralnick, J. A., and Boon, E. M. (2012) Nitric oxide regulation of cyclic di-GMP synthesis and hydrolysis in *Shewanella woodyi*. *Biochemistry 51*, 2087−2099.

(53) Negrerie, M., Cianetti, S., Vos, M. H., Martin, J. L., and Kruglik, S. G. (2006) Photoinduced coordination dynamics of cytochrome *c*: ferrous versus ferric species studied by time-resolved resonance Raman and transient absorption spectroscopies. *J. Phys. Chem. B 110*, 12766−12781.

(54) Beal, D., Rappaport, F., and Joliot, P. (1999) A new high-sensitivity 10-ns time-resolution spectrophotometric technique adapted to in vivo analysis of the photosynthetic apparatus. *Rev. Sci. Instrum. 70*, 202−207.